Scientific Papers. Series A. Agronomy, Vol. LXIV, No. 1, 2021
ISSN 2285-5785; ISSN CD-ROM 2285-5793; ISSN Online 2285-5807; ISSN-L 2285-5785

USE OF MEDIUM AND HIGH-RESOLUTION REMOTE SENSING DATA AND MARKOV CHAINS FOR FORECASTING PRODUCTIVITY OF NON-CONVENTIONAL FODDER CROPS

Tamara MYSLYVA, Branislava SHELIUTA, Vera BUSHUEVA

Belarusian State Agricultural Academy, 5 Michurina Street, Gorki, Mogilev Region, 213407 Republic of Belarus

Corresponding author email: byrty41@yahoo.com

Abstract

This paper provides the results of assessing the possibility of using remote sensing data obtained from the Sentinel-2 with a spatial resolution of 10 m and simple Markov chains to predict the degree of development of Galega orientalis within the local area. The possibility of using remote sensing data obtained with the Phantom-4ProV 2.0 to assess the productivity of Silphium perfoliatum and Zea mays biomass was also evaluated. The studies were carried out in 2017-2020 on the territory of Gorki district (Republic of Belarus). The research indicated that the use of the Markov model and the raster image of the NDVI index as a predictor makes it possible to accurately predict the areas with very poorly developed, poorly developed, moderately developed, developed and well-developed vegetation ($\chi 2_{empiric} = 0.401$; $\chi 2_{critical} = 9.488$). Vegetation indices ExG, VARI, WI, and EXGR, are suitable for creating a predictive multiple linear regression model that allows predicting the productivity of Silphium perfoliatum in the stalking phase with an error not exceeding 2%, while indices RGBVI, ExG and EXGR it is advisable to use for yield predicting of corn (MAPE=5.19%).

Key words: *forecasting, productivity, biomass, remote sensing, UAV.*

INTRODUCTION

Precision agriculture is a modern management concept that uses digital methods to monitor and optimize agricultural production processes (Maloku, 2020). In this regard, like no other industry, it needs high-precision data, of which more than 80% is geospatial data. The most reliable and demanded source of data for precision farming is remote sensing data, the share of which in the structure of precision farming technology elements has a steady tendency to increase on a global scale (Aulbur et al., 2019). In this regard the promising direction is the use of ultrahigh-resolution remote sensing data obtained from UAVs for monitoring and forecasting the productivity of grain and forage crops (Myslyva, 2020). Plant height data obtained from a digital model of the vegetation surface, which is created from the results of aerial photography, is traditionally used in assessing the biomass productivity of spring wheat (Zhaopeng et al., 2020; Hassan, 2019), winter barley (Bendig et al., 2015; 2014), corn (Furukawa et al., 2020; Zhang et al., 2020). For fodder crops, UAV data are used to assess the productivity of pasture grasses (Michez et al., 2019; Barbosa et al., 2019). However, the methodology for performing this type of work differs in the context of individual crops and their growing conditions. Moreover, it needs improvement and adaptation to the specific economic and agroecological conditions of a particular territory.

The most important indicator of the efficiency of the agricultural sector is the volume of crop production and the yield of agricultural crops. Against the background of global climatic changes, reliable forecasting of the productivity of agricultural crops is a rather difficult process, since a number of factors are involved in the formation of the yield. Improving the quality of predictive models is possible through the combined use of various types of data and forecasting techniques. In particular, to predict the yield, the capabilities of neural networks (Crane-Droesch, 2018; Shivnath Ghosh, 2014) and remote sensing data (Khaki & Wang, 2019; Ennouri & Kallel, 2019) are widely used, which provides quick analysis in the state of crops and plantations of agricultural crops over large areas. An effective and at the same time simple way to simulate random events, which includes forecasting the productivity of biomass, is modelling using Markov chains. At present, it is widely used to predict the productivity of various agricultural crops, however, such studies have not previously been performed in Belarus. In this regard, the development of predictive models that make it possible to obtain reliable estimates of crop productivity based on the joint use of remote sensing data and statistical modelling becomes relevant.

In this context, the paper presents the results of assessing the possibility of using remote sensing data with medium and ultra-high resolution and Markov chains for predicting the productivity of *Galega orientalis*, *Silphium perfoliatum* and *Zea mays* in agroecological conditions of the north-eastern part of the Republic of Belarus.

MATERIALS AND METHODS

The studies were carried out in 2017-2020 on the territory of the Gorki district, Mogilev region of the Republic of Belarus. Information about the location of the research objects is shown in Figure 1.

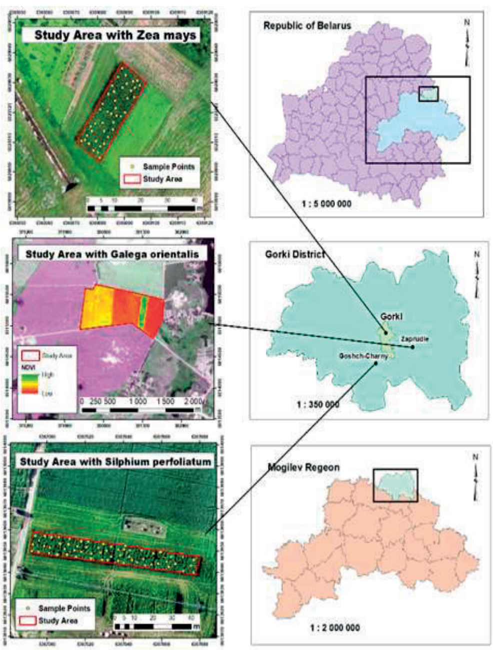

Figure1. Location of the research object

The object of the research was the development and biomass productivity of the following crops:

– *Silphium perfoliatum* L. (common name – cup plant), variety Owari giant (Hungary), development phase – full plant stem phase;

– *Zea mays* L., hybrid Rodriguez (KWS), FAO 170, development phase – R6, V13;

– *Galega orientalis* L. (common name – goat's rue), variety Nesterka (Belarus), development phase – full regrowth after the second cut.

The research was carried out in several stages, the list of which is presented in Figure 2.

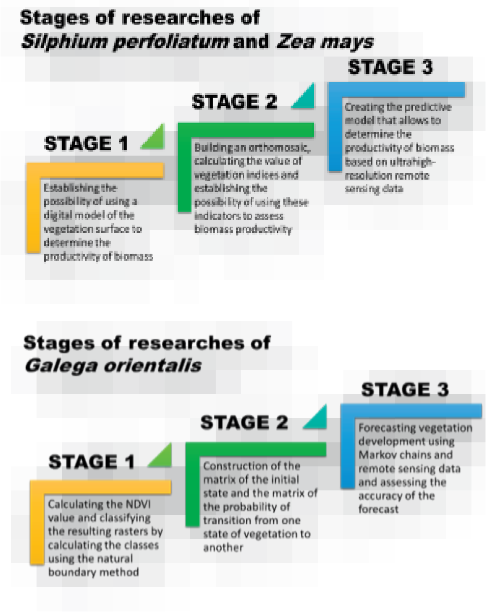

Figure 2. Stages of the researches

The UAV used in this study was quadcopter Phantom-4ProV 2.0. It is equipped with a 20 MPx digital camera with RGB-sensor. Images were captured at 50 m above ground level. Shooting spatial resolution – 2.5 cm; longitudinal and transverse overlap – 80%, the number of images obtained – 236 pcs and 216 respectively. Survey date: June 6, 2020 (*Silphium perfoliatum*) and July 27, 2020 (*Zea mays*).

The flight mission was formed using the Drone Deploy software product. Aerial photography data processing, elevation mapping and orthomosaic creation were performed using Agisoft PhotoScan Professional software.

The vegetation indices were calculated using the QGIS 3.16. The following indices were calculated: RGBVI (Red Green Blue Vegetation

Index), GLI (Green Leaf Index), VARI (Visible Atmospherically Resistant Index), NGRDI (Normalized Green-Red Difference Index) (Bendig et al., 2015); ExG (Excess Green Index), WI (Woebbecke Index) (Woebbecke et al., 1995); EXGR (Excess Green-Red Index) (Meyer & Neto, 2008); VEG (Vegetativen) (Marchant & Onyango, 2000); CIVE (Color Index of Vegetation) (Kataoka et al., 2003); COMB1 (Combined Index 1), COMB2 (Combined Index 2), GR (Ratio Green/Red Index), SAVI (Soil Adjusted Vegetation Index) (Beniaich et al., 2019).

On the day of the survey, 60 biomass samples of silphium and 42 samples of corn were randomly selected to verify the results within the study area in the field. The sampling sites were coordinated using GPS positioning. For each sample taken, its length in cm, weight in kg and density in kg/m^3 were determined.

To predict the development of plants, the methodological approaches outlined in the works of Chinese scientists (Li & Zhu, 2018) were used in relation to forecasting types of land use. A simple Markov chain, taking into account the correlation between adjacent members of the series, was used to predict the degree of development of the *Galega orientalis*. The prediction is based on the calculation of the transition matrix, the elements of which are the probabilities of transition of the predicted parameters from one state to another, from one value to another.

As a source of geospatial data with medium resolution, three scenes obtained from satellites Sentinel 2A (October 2017) and Sentinel 2B (October 2018, 2019) with a spatial resolution of 10 m (datum – WGS-84, map projection UTM 36N, processing level – 1C) were used.

The degree of vegetation cover development was assessed by the value of the vegetation index NDVI (Normalised Difference Vegetation Index) (Jinru & Baofeng, 2017).

Remote sensing data were processed using the functionality of ArcGIS version 10.5. The classification of rasters with vegetation index NDVI was carried out using the method of principal components.

Statistical processing of the obtained results, construction of regression models and their cross-validation were performed in the Statistica 13.0 (TIBCO Software Inc.).

RESULTS AND DISCUSSIONS

At the first stage, crop surface model (CSM) in *tif image format with a resolution of 2.5 cm was obtained after processing the results of aerial photography. The minimum height of the constructed surface of silphium plant heights was 143.64 cm, the maximum – 144.66 cm, average – 144.17 cm, standard deviation – 0.18 cm. For maize the minimum height of the CSM was 161.59 cm, the maximum – 164.25 cm, average – 163.06 cm, standard deviation – 0.67 cm. To obtain plant heights, the difference between the vegetation heights obtained from the surface model raster and the minimum height determined within the raster was found.

The raster image of the surface model of the silphia vegetation cover was reclassified into 11 classes, since the minimum determined plant height was 0.1 m, and the maximum - 1.1 m with a step of 0.1 m. The raster image of the surface model of the maize vegetation cover was reclassified into 6 classes with a step of 0.01 m. Further, the area occupied by plants with different heights within the study area was determined, and the productivity of the biomass was calculated (Figure 3).

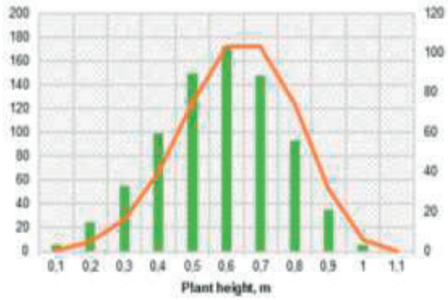

a) *Silphium perfoliatum*

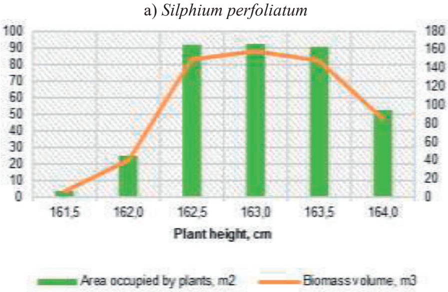

b) *Zea mays*

Figure 3. Productivity of *Silphium perfoliatum* (a) and *Zea mays* (b) biomass, determined from the data of the UAV survey

The minimum yield of raw silphia biomass was 1.49 t·ha^{-1}, the maximum – 16.4 t·ha^{-1}, and the weighted average yield was 8.63 t·ha^{-1}, while for dry biomass the minimum, maximum and weighted average yields reached 0.29 t·ha^{-1}, 3.15 t·ha^{-1} and 1.72 t·ha^{-1}, respectively.
The following results were obtained for maize: the minimum yield of raw biomass was 2.72 t·ha^{-1}, the maximum – 16.63 t·ha^{-1}, and the weighted average yield was 11.66 t·ha^{-1}, while for dry biomass the minimum, maximum and weighted average yields reached 0.82 t·ha^{-1}, 4.98 t·ha^{-1} and 3.49 t·ha^{-1}, respectively.
To determine the reliability of the assessment of biomass productivity, the actual plant height measured in the field was compared with the data obtained using the UAV, and the plant productivity was determined, calculated from the actual and predicted heights. It was found that the results obtained are in fairly good agreement with each other, and their relationship is described by a linear relationship. The correlation coefficient between the actual and predicted values of the productivity of silphia and maize was 0.98 and 0.89, and the average approximation error was 3.3 and 4.9%, respectively, which indicates the reliability of the established dependencies (Figure 4).

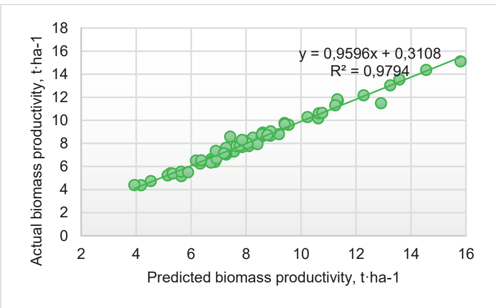

a) *Silphium perfoliatum*

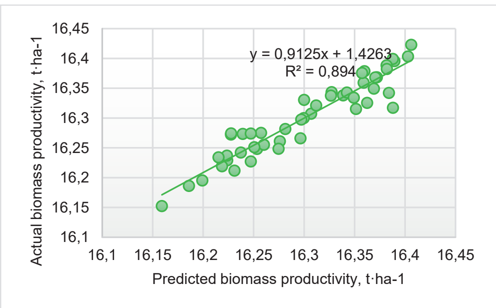

b) *Zea mays*

Figure. 4. The relationship between the actual and predicted biomass productivity

At the second stage of the researches, the possibility of using data on the value of vegetation indices for assessing biomass productivity was assessed. Vegetation indices were calculated using normalized RGB channels. The RGB bands were converted into normalized forms using the following Equation (1) (Yahui et al., 2020):

$$R=r\div(r+g+b);\ G=g\div(r+g+b);\ B=b\div(r+g+b),$$

where r, g, and b are the original digital values from the RGB images.
For silphia, the average values of the vegetation indices RGBVI, NDRGI, and GLI, as well as the vegetation indices SAVI and ExG, were quite similar to each other, while the average values of the GR and VEG indices had the highest values. At the same time, for maize, the maximum mean values were observed for the vegetation indices CIVE, COMB 1 and COMB 2, and the mean values of GLI and VARI, as well as NDRGI and SAVI, were similar to each other (Figure 5).

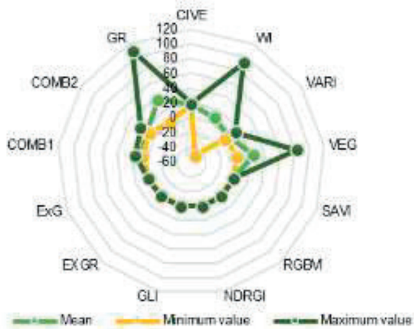

a) *Silphium perfoliatum*

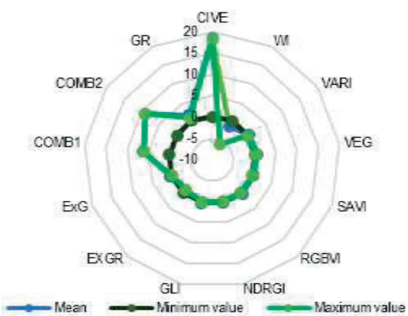

b) *Zea mays*

Figure. 5. Statistical characteristics of the values of vegetation indices obtained from the orthomosaic created on the basis of UAV imagery in RGB

However, the results of assessing the relationship between the values of vegetation indices and biomass productivity indicate that, despite the similarity of the absolute values, these vegetation indices are characterized by varying degrees of relationship with the productivity of silphia and maize biomass (Table 1–2).

Table 1. The relationship between the values of the vegetation indices obtained from the orthomosaic and the raw biomass productivity of *Silphium perfoliatum*, n = 60

Vegetation index	R^2	RMSE, $t \cdot ha^{-1}$	MAPE, %
ExG	0.95	1.08	20.5
RGBVI	0.94	1.12	27.0
NGRDI	0.94	1.12	20.7
EXGR	0.93	1.22	23.2
CIVE	0.91	1.40	15.9
WI	0.90	1.47	19.3
GR	0.89	1.51	30.2
GLI	0.87	1.68	38.5
VEG	0.83	1.94	39.1
COMB1	0.78	2.23	44.7
COMB2	0.78	2.20	43.7
VARI	0.66	2.74	43.7
SAVI	0.44	3.53	58.7

Table 2. The relationship between the values of the vegetation indices obtained from the orthomosaic and the raw biomass productivity of *Zea mays*, n = 42

Vegetation index	R^2	RMSE, $t \cdot ha^{-1}$	MAPE, %
ExG	0.90	1.58	13.5
RGBVI	0.62	3.58	29.6
NGRDI	0.87	1.82	16.2
EXGR	0.85	1.98	21.9
CIVE	0.81	2.53	25.2
WI	0.95	1.41	12.5
GR	0.89	1.75	14.6
GLI	0.71	3.25	18.4
VEG	0.92	1.51	13.1
COMB1	0.76	2.59	15.6
COMB2	0.76	2.20	15.2
VARI	0.65	3.21	29.4
SAVI	0.56	3.87	33.3

In particular, the strongest direct linear relationship with the productivity of silphia plants was established for the ExG, RGBVI, NGRDI indices, while the productivity of maize biomass was closely related to the WI, VEG, and ExG indices. The VARI and SAVI indices are characterized by the least dependence on the biomass productivity of both silphia and maize. It should be noted that the high information content of the ExG vegetation index is also indicated by (Beniaich et al., 2019; Tumlisan, 2017), and the RGBVI index, by (Bendig et al., 2015). The SAVI vegetation index is most suitable for distinguishing between vegetated and open soil areas, however, like the combined COMB1 and COMB2 indices, it is not informative enough for assessing biomass productivity. Its low indicator capacity is also evidenced by the results of the study presented by Zhaopeng et al., 2020. The results obtained also correlate with the data of Michez et al., 2019, in which, when establishing the possibility of using vegetation indices RGBVI, GLI, NGRDI and VARI to assess the biomass productivity of meadow grasses the root-mean-square error of the estimate was 6.02 $t \cdot ha^{-1}$, 5.04 $t \cdot ha^{-1}$, 1.93 $t \cdot ha^{-1}$ and 1.42 $t \cdot ha^{-1}$, respectively.

The calculation of the average approximation error indicates that, despite the presence of a rather strong direct linear relationship between the values of individual vegetation indices and the productivity of silphia and maize biomass, the use of any one index for a reliable assessment of the productivity level of these crops is not possible, since even for the most of informative indices, the average approximation error reached 16–27% and 12–14%, respectively. In this regard, the third stage of the study was to establish the possibility of using a complex of vegetation indices to determine the productivity of biomass by performing stepwise multiple regression. As a result, a regression model of the following form was obtained (2):

$$y = -317.181 + 0.997 \cdot WI - 4.702 \cdot VARI - 389.566 \cdot EXGR + 417.682 \cdot ExG$$

The mean absolute percentage error of this model was 1.82%, the average error (SE) was 0.18 $t \cdot ha^{-1}$, and the root mean square (RMSE) was 0.13 $t \cdot ha^{-1}$, which indicates its high reliability and suitability for monitoring biomass productivity of *Silphium perfoliatum* in the full plant stem phase.

A regression model of the following type was obtained for corn (3):

$$y = 16.558 - 0.135 \cdot RGBVI + 0.119 \cdot ExG - 0.097 \cdot EXGR$$

The mean absolute percentage error of this model was 5.19%, the average error (SE) was 0.81 $t \cdot ha^{-1}$, and the root mean square (RMSE) was 2.30 $t \cdot ha^{-1}$, which indicates its high reliability and suitability for monitoring the productivity of *Zea mays* biomass in the R6 V13 phase.

The prognosis of the development of the vegetation cover represented by

Galega orientalis and the assessment of its effectiveness were also carried out in several successive stages. At the first stage, the calculation of the Normalized Difference Vegetation Index, NDVI was carried out (Myslyva et al., 2020), and raster images of the vegetation cover were obtained at different time periods (Figure 6).

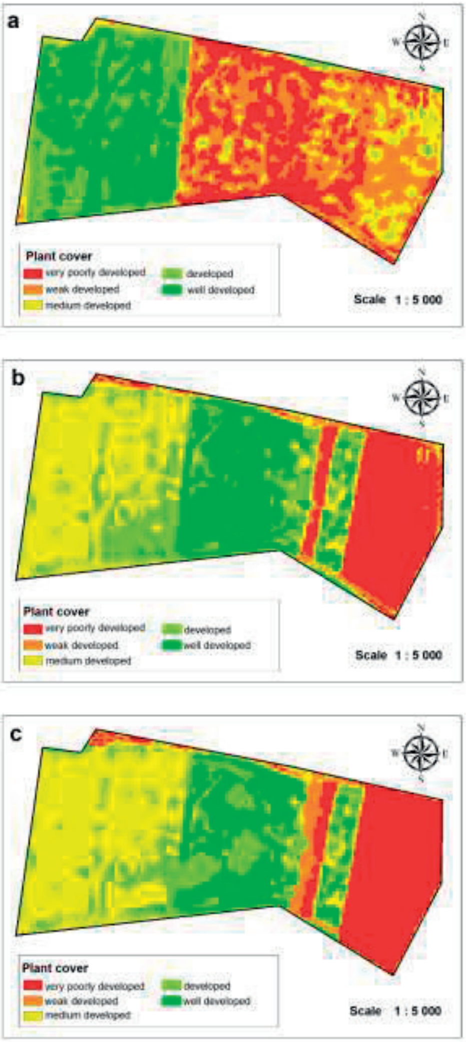

Figure. 6. Raster images of the vegetation index NDVI: a – 2017, b – 2018; c – 2019

The resulting rasters were classified according to the method of principal components. Furthermore, they were differentiated by the NDVI value by calculating the classes by the method of natural boundaries. The intervals of values of the vegetation index corresponding to one or another degree of development of the vegetation cover in the studied area are presented in Table 3.

Table 3. Intervals of vegetation index values corresponding to the degree of vegetation cover development

Plant development level	Range of NDVI values
Very poorly developed	0.15–0.30
Weak developed	0.31–0.36
Medium developed	0.37–0.50
Developed	0.51–0.60
Well developed	0.61–0.77

The transformation of the obtained raster images into vector layers made it possible to determine the areas within the raster, corresponding to one or another level of plant development (Table 4).

Table 4. Distribution of areas with different degrees of vegetation development (based on the results of determining the value of the vegetation index NDVI), %

Year	Plant development level				
	very poorly developed	weak developed	medium developed	developed	well developed
2017	20.84	27.07	12.56	16.62	22.91
2018	19.39	5.81	31.23	18.73	24.82
2019	25.48	23.46	41.08	5.083	4.88

The rasters of 2017 and 2018 were used for the prediction, and the raster of 2019 served as a basis to assess the accuracy of the prediction.
The initial state matrix S(0) was constructed based on the data presented in the Tables 3 and 4 (4):

$$S(0) = \begin{bmatrix} 17.67 \\ 22.95 \\ 10.65 \\ 14.09 \\ 19.42 \end{bmatrix} = \begin{bmatrix} NDVI - & 0.15 - & 0.30 \\ NDVI - & 0.31 - & 0.36 \\ NDVI - & 0.37 - & 0.50 \\ NDVI - & 0.51 - & 0.60 \\ NDVI - & 0.61 - & 0.77 \end{bmatrix}$$

The next stage of the research was the construction of a matrix of the probability of vegetation transition from one state to another. To achieve this goal, the rasters of 2017 and 2018 were overlaid and the areas of their mutual intersection were determined. Further, the obtained values were transformed into a matrix of transition of areas with different degrees of plant development. The matrix of the transition of areas in hectares was recalculated into the matrix of the probability of transitions of areas with different degree of development of vegetation cover in one class or another (Table 5).

Table 5. Matrix of probability of transitions of areas with different degrees of vegetation development (n = 0)

2017	2018				
	Plant development level				
	very poorly developed	weak developed	medium developed	developed	well developed
Very poorly developed	0.143875	0.528585	0.322489	0.005051	0
Weak developed	0.184886	0.370909	0.323199	0.112836	0.008169
Medium developed	0.0544338	0.034638	0.031049	0.412253	0.467626
Developed	0.226778	0.148231	0.049930	0.145621	0.429439
Well developed	0.443318	0.449301	0.087082	0.003237	0.017062

At the final stage, the forecast for the development of galega in 2019 was carried out. For its implementation, the matrix of the initial state and the matrix of the probability of transition from one state to another were used. The actual and predicted values of the areas with varying degrees of vegetation development were used to assess the accuracy of the forecast, while the χ^2 criterion was used to test the forecast model (Table 6).

Table 6. Results of estimation of accuracy of the forecast model of vegetation cover development, hectares

Plant development level	Predicted value (Y')	Actual value (Y)	Absolute error (Y' – Y)	$(Y' – Y)^2$
Very poorly developed	21.61	19.26	–2.35	5.54
Weak developed	19.89	20.35	0.46	0.21
Medium developed	34.83	32.22	–2.61	6.83
Developed	4.31	9.07	4.76	22.62
Well developed	4.14	6.78	2.64	6.98
$\chi^2_{empirical} = 0.401$; $\chi^2_{critical} = 9.488$				

The maximum value of the absolute error is typical for forecasting areas with medium developed, developed and well-developed vegetation. This phenomenon can be explained by the fact that in the process of recognizing rasters with the vegetation index NDVI by the method of principal components it is rather difficult to distinguish these classes, since their spectral brightness is in a rather close range of values. However, it is possible to improve the quality of recognition by performing preliminary raster segmentation and then applying machine learning to classify it.

CONCLUSIONS

The results obtained give reason to recommend the use of ultra-high-resolution remote sensing data obtained from UAVs to assess the biomass productivity of *Silphium perfoliatum* and *Zea mays*.

Plant height data obtained from an aerial-based crop surface model is suitable for use in estimating the productivity of silphia and maize biomass: the R^2 for the relationship between actual productivity and remotely sensed productivity is 0.98 and 0.89, respectively.

Predictive models created by the method of stepwise multiple linear regression, including a complex of several vegetation indices, make it possible to determine the silphia and maize biomass productivity according to ultra-high-resolution remote sensing data with an error of no more than 2-5%.

Medium resolution remote sensing data obtained with the Sentinel 2 and the functionality of GIS technologies allow creating adequate models using Markov chains for predicting the development of *Galega orientalis* in local areas.

The process of predicting the productivity of galega plants using Markov chains should include such stages as: obtaining a raster image; raster classification and converting it to vector layer; construction of an initial state matrix and a transition probability matrix.

Further research should focus on assessing the validity of the resulting models in the field. The results of this study can be useful both in the development of forecasting methodology and in direct forecasting of the biomass productivity of *Silphium perfoliatum*, *Zea mays* and other fodder crops, in particular *Helianthus annuus* and *Helianthus tuberosus*, as well as for assessing the productivity of pastures and creating effective pasture crop rotations.

REFERENCES

Aulbur, W., Henske, R., Uffelmann, W., Schelfi, G. (2019). *Farming 4.0: How precision agriculture might save the world*. Munich: Roland Berger GMBH.

Barbosa, B.D.S., Ferraz, G.A.S., Gonçalves, L.M., Marin, D.B., Maciel, D.T., Ferraz, P.F.P., Rossi, G. (2019). RGB vegetation indices applied to grass monitoring: a qualitative analysis. *Agronomy Research*, *17*(2), 349–357.

Bendig, J., Bolten, A., Bennertz, S., Broscheit, J., Eichfuss, S., Bareth, G. (2014). Estimating biomass of barley using crop surface models (CSMs) derived from UAV-based RGB imaging. *Remote Sensing*, *6*. 10395–10412.

Bendig, J., Kang Y., Aasena, H., Bolten, A., Bennertz, S., Broscheit, J... (2015). Combining UAV-based plant height from crop surface models, visible, and near infrared vegetation indices for biomass monitoring in barley. *International Journal of Applied Earth Observation and Geoinformation*, *39*. 79–87.

Beniaich, A., Leandro Naves Silva, M., Arnaldo Pomar Avalos, F., Duarte de Menezes, M., Moreira Candido B. (2019). Determination of vegetation cover index under different soil management systems of cover plants by using an unmanned aerial vehicle with an onboard digital photographic camera. *Ciências Agrárias*, *40*(1), 49–66.

Crane-Droesch, A. (2018). Machine learning methods for crop yield prediction and climate change impact assessment in agriculture. *Environmental Research Letters*, *13*(11), 1–26.

Ennouri, K., Kallel, A. (2019). Remote sensing: an advanced technique for crop condition assessment. *Mathematical Problems in Engineering*, *1*. 1–8.

Furukawa, F., Maruyama, K., Saito, Y., Kaneko, M. (2020). Corn height estimation using UAV for yield prediction and crop monitoring. In R. Avtar, T. Watanabe, *Unmanned Aerial Vehicle: Applications in Agriculture and Environment* (pp. 51-69). Springer: Berlin/Heidelberg, Germany.

Hassan, M.A., Mengjiao, Y., Luping, Fu., Rasheed, A., Bangyou, Z., Xianchun, Xia…(2019). Accuracy assessment of plant height using an unmanned aerial vehicle for quantitative genomic analysis in bread wheat. *Plant Methods*, *15*. 37.

Jinru, X., Baofeng, Su. (2017). Significant remote sensing vegetation indices: a review of developments and applications. *Journal of Sensors*. Retrieved from https://www.hindawi.com/journals/js/2017/1353691/

Kataoka, T., Kaneko, T., Okamoto, H., Hata, S. (2003). Crop growth estimation system using machine vision. *Proceedings 2003 IEEE/ASME International Conference on Advanced Intelligent Mechatronics*, Kobe, *2*(1), 1079–1083.

Khaki, S., Wang, L. (2019). Crop yield prediction using deep neural networks. *Frontiers in Plant Science*, *10*, 1–10.

Li, B., Zhu, X. (2018). Forecast of maize production in Henan province. *American Journal of Plant Sciences*, *9*, 2276–2286.

Maloku, D. (2020). Adoption of precision farming technologies: USA and EU situation. *Practical Application of Science*, *VIII*(22), 7–14.

Marchant, J.A., Onyango, C.M. (2000). Shadow invariant classification for scenes illuminated by daylight. *Journal of the Optical Society of America*, *17*(11), 1952–1961.

Meyer, G.E., Neto, J.C. (2008). Verification of colour vegetation indices for automated crop imaging applications. *Computers and Electronics in Agriculture*, *63*(2), 282–293.

Michez, A., Lejeune, P., Bauwens, S., Herinaina, A.A.L., Blaise, Y., Castro, Muñoz E., Lebeau, F., Bindelle, J. (2019). Mapping and monitoring of biomass and grazing in pasture with an Unmanned Aerial System. *Remote Sensing*, *11*(5), 473.

Myslyva, T. (2020). Problems, prospects and experience in the implementation of precision farming in the Republic of Belarus in the context of national land use. *Proceedings of the XI International Scientific Agricultural Symposium*, East Sarajevo, 972–978.

Myslyva, T.N., Bushueva, V.I., Valyntsava, V.A. (2020). Assessment of possibility for using remote sensing data and Markov chains for prediction of vegetation cover development. *Proceedings of the National Academy of Sciences of Belarus, 58*(2), 176–184.

Shivnath Ghosh, S.K. (2014). Machine learning for soil fertility and plant nutrient management. *International Journal on Recent and Innovation Trends in Computing*, *2*(2), 292–297.

Tumlisan, G.Y. (2017). Monitoring growth development and yield estimation of maize using very high-resolution UAV-images in Gronau, Germany. Thesis (Master). Enschede, University of Twente.

Woebbecke, D.M., Meyer, G.E., Von Bargen, K., Mortensen, D.A. (1995). Colour indexes for weed identification under various soil, residue, and lighting conditions. *Transactions of the ASAE*, *38*(1), 259–269.

Yahui, G., Hanxi, W., Zhaofei, Wu., Shuxin, W., Hongyong, S., Senthilnath, J., Jingzhe, W., Robin, B.C., Yongshuo, Fu. (2020). Modified red blue vegetation index for chlorophyll estimation and yield prediction of maize from visible images captured by UAV. *Sensors*, *20.* 5055.

Zhang, M., Zhou, J., Kenneth, S.A., Newell Kitchen, R. (2020). Estimation of maize yield and effects of variable- rate nitrogen application using UAV-based RGB imagery. *Biosystems Engineering*, *189*. 24–35.

Zhaopeng, Fu, Jie, J., Yang, Gao, Krienke, B., Meng W., Kaitai, Z.… (2020). Wheat growth monitoring and yield estimation based on multi-rotor unmanned aerial vehicle. *Remote Sensing*, *12*. 508.